

Modelling of a cyclist’s power for time trials on a velodrome

Len Bos*, Michael A. Slawinski†, Raphaël A. Slawinski‡, Theodore Stanoev§

Abstract

We formulate a phenomenological model to study the power applied by a cyclist on a velodrome—for individual timetrials—taking into account the straights, circular arcs, connecting transition curves and banking. The dissipative forces we consider are air resistance, rolling resistance, lateral friction and drivetrain resistance. Also, the power is used to increase the kinetic and potential energy. Herein, to model a steady ride—as expected for individual timetrials—we assume a constant centre-of-mass speed, while allowing the cadence and power to vary during a lap. Hence, the kinetic energy is constant and the only mechanical energy whose change we need to consider is the increase of potential energy due to raising the centre of mass upon exiting each curve. The effect of dissipative forces is examined at each point of the lap; the effect of conservative forces is examined as an average. The latter, albeit not negligible, is a small part of the total power.

Following derivations and justifications of expressions that constitute this mathematical model, we present a numerical example. We show that the cadence and power vary only slightly during a steady ride. In other words, a constant centre-of-mass speed entails nearly constant cadence and power, as expected for a steady ride.

Also, we examine changes in the required power due to changes of various quantities, such as air density at a velodrome, laptime and several others, as well as the model sensitivity to input errors. Furthermore, we examine the effects on required power of slight and gradual changes of speed, which are pertinent to individual time trials.

Such examinations are of immediate use in strategizing the performance for individual pursuits and the Hour Record, as well as in evaluating agreements between models and measurements since both are subject to inaccuracies and errors. Notably, scenarios generated with our model were taken into consideration prior to two successful Hour Records in 2022: Daniel Bigham and Filippo Ganna.

1 Introduction

In this article, we formulate a mathematical model to examine the power expended by a cyclist on a velodrome. The model includes several simplifying assumptions that permit the derivation of closed-form expressions, while nevertheless capturing the mechanical behavior in an empirically adequate manner. The assumptions pertain to both the bicycle-cyclist system and the design of the track.

For the former, we assume the cyclist to be already in a launched effort, which renders the model adequate for longer events, such as a 4000-metre pursuit or, in particular, the Hour Record. Limiting our attention to a steady ride, we view its motion as tantamount to a constant centre-of-mass speed. To consider the effect of leaning, we distinguish between the centre-of-mass and wheel speeds to decompose the forces that act on various parts of the bicycle-cyclist system throughout a given lap.

*Università di Verona, Italy, leonardpeter.bos@univr.it

†Memorial University of Newfoundland, Canada, msslawins@mac.com

‡Mount Royal University, Canada, rslawinski@mtroyal.ca

§Memorial University of Newfoundland, Canada, theodore.stanoev@gmail.com

We determine the lean angles by assuming the system is in instantaneous rotational equilibrium about the line of contact with the tires on the ground, which is tantamount to net zero torque.

For the latter, geometrically, we consider a velodrome with its straights, circular arcs and connecting transition curves, whose inclusion — as indicated by Fitzgerald et al. (2021) — has been commonly neglected in previous studies. While this inclusion presents a mathematical challenge, it increases the empirical adequacy of the model. We consider that the black line, which is the curve at a fixed distance from the inner edge of the track — along which the distance is measured — is adequately represented by a line confined to the horizontal plane, even though it is not exactly so. Also, we assume the cyclist trajectory to coincide with that line. All in all, we focus our attention on phenomenological quantities that affect the bicycle-cyclist system, with a particular emphasis on the required power.

Various power models and velodrome geometries have been presented in previous studies. Almost a quarter-of-a-century ago, Martin et al. (1998) formulate and examine a road-cycling model. Proceeding with velodrome models, Underwood and Jermy (2010, 2014) formulate and examine a model for individual pursuits that includes leaning on the bends, but only uses straights and bends without transition curves. Lukes et al. (2012) model the power of a cyclist on a velodrome, including the tire scrubbing effects. Fitton and Symons (2018) present a model that includes slip and steering angles and variable black-line altitude, and use velodrome models based on theodolite measurements.

Most recently, Fitzgerald et al. (2021) quantify the effects of transition curves on a power model consistent with Lukes et al. (2012) and Martin et al. (1998). They consider two types of transition curves, namely, a twice-differentiable linear increase in curvature, which is the Euler spiral, and a sinusoid, which exhibits a continuous derivative of curvature. The effects of these curves are estimated using least squares optimization of black-line measurements obtained with theodolite measurements.

We begin this article by expressing mathematically the geometry of both the black line and the inclination of the track. We provide a detailed derivation of the Euler spiral, which already appeared as an earlier version of this arXiv and was referred to by Fitzgerald et al. (2021) as the most detailed to date. Also, we derive a Bloss-transition curve, whose curvature is thrice-differentiable. Our expressions are accurate representations of the common geometry of modern 250-metre velodromes, whose design details were provided by Mehdi Kordi (*pers. comm.*, 2020). We proceed to formulate an expression for power used against dissipative forces and power used to increase mechanical energy. In particular, while earlier work considers changes in potential energy as a function of vertical location on a banked velodrome (e.g., Benham et al. (2020)) or of the lean angle and the vertical inclination of trajectory (e.g., Fitton and Symons (2018)), we consider — in accordance with the assumption of instantaneous rotational equilibrium — increases in potential energy due solely to straightening of the cyclist upon exiting the curves, with wheels remaining along the black line. We show that a significant amount of power is expended in that process. To present a numerical example and for a comparison with Fitzgerald et al. (2021), we examine the case of a constant centre-of-mass speed, which we consider the best mathematical analogy for steadiness of timetrial efforts on a velodrome. As the final point of this article, we consider the applicability of our formulation to model changes of speed. For completeness, we include appendices, where we present derivations of expressions for the air resistance and lean angle, change of potential energy with the lean angle, effects of gradual speed increase, and a brief discussion of empirical adequacy of model assumptions.

2 Track

2.1 Black-line parameterization

To model the required power of a cyclist who follows the black line, in a constant aerodynamic position, as illustrated in Figure 1, we define this line by three parameters.

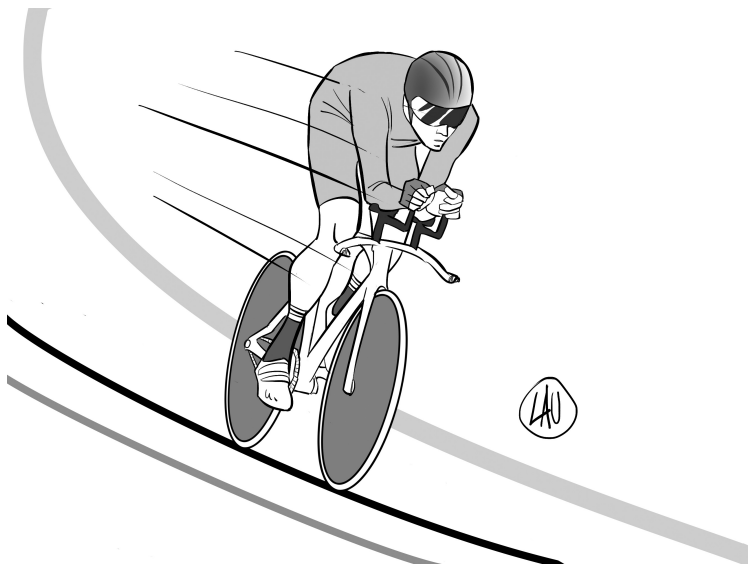


Figure 1: A constant aerodynamic position along the black line

- L_s : the half-length of the straight
- L_t : the length of the transition curve between the straight and the circular arc
- L_a : the length of the remainder of the quarter circular arc

The length of the track is $S = 4(L_s + L_t + L_a)$. In Figure 2, we show a quarter of a black line for $L_s = 19$ m, $L_t = 13.5$ m and $L_a = 30$ m, which results in $S = 250$ m. This curve has continuous

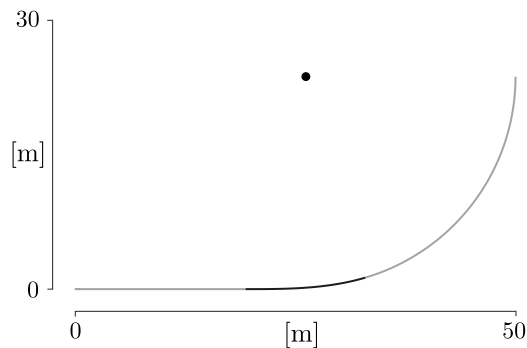


Figure 2: A quarter of the black line for a 250-metre track

derivative up to order two; it is a C^2 curve, whose curvature is continuous.

To formulate, in Cartesian coordinates, the curve shown in Figure 2, we consider the following.

- The straight,

$$y_1 = 0, \quad 0 \leq x \leq a,$$

shown in gray, where $a := L_s$.

- The transition, shown in black—following a standard design practice—we take to be an Euler spiral, which can be parameterized by Fresnel integrals,

$$x_2(\varsigma) = a + \sqrt{\frac{2}{A}} \int_0^{\varsigma\sqrt{\frac{A}{2}}} \cos(x^2) dx \quad \text{and} \quad y_2(\varsigma) = \sqrt{\frac{2}{A}} \int_0^{\varsigma\sqrt{\frac{A}{2}}} \sin(x^2) dx,$$

with $A > 0$ to be determined; herein, ς is the curve parameter. Since the arclength differential, ds , is such that

$$ds = \sqrt{x_2'(\varsigma)^2 + y_2'(\varsigma)^2} d\varsigma = \sqrt{\cos^2\left(\frac{A\varsigma^2}{2}\right) + \sin^2\left(\frac{A\varsigma^2}{2}\right)} d\varsigma = d\varsigma,$$

we write the transition curve as

$$(x_2(s), y_2(s)), \quad 0 \leq s \leq b := L_t.$$

- The circular arc, shown in gray, whose centre is (c_1, c_2) and whose radius is R , with c_1, c_2 and R to be determined. Since its arclength is specified to be $c := L_a$, we may parameterize the quarter circle by

$$x_3(\theta) = c_1 + R \cos(\theta) \tag{1}$$

and

$$y_3(\theta) = c_2 + R \sin(\theta), \tag{2}$$

where $-\theta_0 \leq \theta \leq 0$, for $\theta_0 := c/R$. The centre of the circle is shown as a black dot in Figure 2.

We wish to connect these three curve segments so that the resulting global curve is continuous along with its first and second derivatives. This ensures that the curvature of the track is also continuous.

To do so, let us consider the connection between the straight and the Euler spiral. Herein, $x_2(0) = a$ and $y_2(0) = 0$, so the spiral connects continuously to the end of the straight at $(a, 0)$. Also, at $(a, 0)$,

$$\frac{dy}{dx} = \frac{y_2'(0)}{x_2'(0)} = \frac{0}{1} = 0,$$

which matches the derivative of the straight line. Furthermore, the second derivatives match, since

$$\frac{d^2y}{dx^2} = \frac{y_2''(0)x_2'(0) - y_2'(0)x_2''(0)}{(x_2'(0))^2} = 0,$$

which follows, for any $A > 0$, from

$$x_2'(\varsigma) = \cos\left(\frac{A\varsigma^2}{2}\right), \quad y_2'(\varsigma) = \sin\left(\frac{A\varsigma^2}{2}\right) \tag{3}$$

and

$$x_2''(\varsigma) = -A\varsigma \sin\left(\frac{A\varsigma^2}{2}\right), \quad y_2''(\varsigma) = A\varsigma \cos\left(\frac{A\varsigma^2}{2}\right).$$

Let us consider the connection between the Euler spiral and the arc of the circle. In order that these connect continuously,

$$(x_2(b), y_2(b)) = (x_3(-\theta_0), y_3(-\theta_0)),$$

we require

$$x_2(b) = c_1 + R \cos(\theta_0) \iff c_1 = x_2(b) - R \cos\left(\frac{c}{R}\right) \quad (4)$$

and

$$y_2(b) = c_2 - R \sin(\theta_0) \iff c_2 = y_2(b) + R \sin\left(\frac{c}{R}\right). \quad (5)$$

For the tangents to connect continuously, we invoke expression (3) to write

$$(x'_2(b), y'_2(b)) = \left(\cos\left(\frac{A b^2}{2}\right), \sin\left(\frac{A b^2}{2}\right) \right).$$

Following expressions (1) and (2), we obtain

$$(x'_3(-\theta_0), y'_3(-\theta_0)) = (R \sin(\theta_0), R \cos(\theta_0)),$$

respectively. Matching the unit tangent vectors results in

$$\cos\left(\frac{A b^2}{2}\right) = \sin\left(\frac{c}{R}\right), \quad \sin\left(\frac{A b^2}{2}\right) = \cos\left(\frac{c}{R}\right). \quad (6)$$

For the second derivative, it is equivalent—and easier—to match the curvature. For the Euler spiral,

$$\kappa_2(s) = \frac{x'_2(s)y''_2(s) - y'_2(s)x''_2(s)}{\left((x'_2(s))^2 + (y'_2(s))^2\right)^{\frac{3}{2}}} = A s \cos^2\left(\frac{A s^2}{2}\right) + A s \sin^2\left(\frac{A s^2}{2}\right) = A s,$$

which is indeed the defining characteristic of an Euler spiral: the curvature grows linearly in the arclength. Hence, to match the curvature of the circle at the connection, we require

$$A b = \frac{1}{R} \iff A = \frac{1}{b R}.$$

Substituting this value of A in equations (6), we obtain

$$\begin{aligned} \cos\left(\frac{b}{2R}\right) &= \sin\left(\frac{c}{R}\right), \quad \sin\left(\frac{b}{2R}\right) = \cos\left(\frac{c}{R}\right) \\ \iff \frac{b}{2R} &= \frac{\pi}{2} - \frac{c}{R} \\ \iff R &= \frac{b + 2c}{\pi}. \end{aligned}$$

It follows that

$$A = \frac{1}{b R} = \frac{\pi}{b(b + 2c)};$$

hence, the continuity condition stated in expressions (4) and (5) determines the centre of the circle, (c_1, c_2) .

For the case shown in Figure 2, the numerical values are $A = 3.1661 \times 10^{-3} \text{ m}^{-2}$, $R = 23.3958 \text{ m}$, $c_1 = 25.7313 \text{ m}$ and $c_2 = 23.7194 \text{ m}$. The complete track—with its centre at the origin, $(0, 0)$ —is shown in Figure 3. The corresponding track curvature is shown in Figure 4. Note that the curvature transitions linearly from the constant value of straight, $\kappa = 0$, to the constant value of the circular arc, $\kappa = 1/R$.

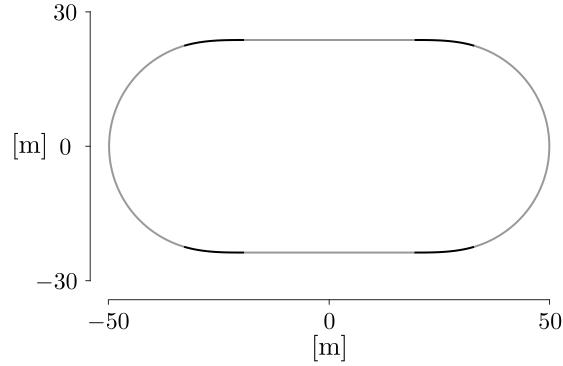


Figure 3: Black line of 250-metre track

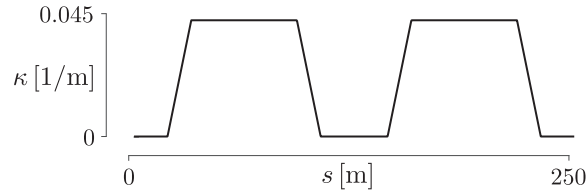


Figure 4: Curvature of the black line, κ , as a function of distance, s , with a linear transition between the zero curvature of the straight and the $1/R$ curvature of the circular arc

2.2 C^3 transition curve

As stated by Fitzgerald et al. (2021),

[t]here can be a trade-off between good spatial fit (low continuity for matching a built velodrome) and a good physical fit (high continuity for matching a cyclist’s path). If this model is used to calculate the motion of cyclists on a velodrome surface then a spatial fit can be prioritised. However, if it is used to directly model the path of a cyclist then higher continuity is required.

Should it be desired that the trajectory have continuous derivatives up to order $r \geq 0$ —which makes it in class C^r , so that its curvature is of class C^{r-2} —it is possible to achieve this by a transition curve $y = p(x)$, where $p(x)$ is a polynomial of degree $2r - 1$ and the solution of a 4×4 system of nonlinear equations, assuming a solution exists.

In case $r = 2$, this would correspond to a transition by a polynomial of degree $2r - 1 = 3$, often referred to as a cubic spiral. In case $r = 3$, this would correspond to a transition by a polynomial of degree $2r - 1 = 5$, often referred to as a Bloss transition.

To see how to do this, for simplicity’s sake, let $a = L_s$. We use a Cartesian formulation, namely,

- $y = 0, 0 \leq x \leq a$: the halfstraight
- $y = p(x), a \leq x \leq X$: the transition curve between the straight and circular arc
- $y = c_2 - \sqrt{R^2 - (x - c_1)^2}$: the end circle, with centre at (c_1, c_2) and radius R .

Herein, $x = X$ is the point at which the polynomial transition connects to the circle, $(x - c_1)^2 + (y - c_2)^2 = R^2$.

X , c_1 , c_2 and R are *a priori* unknowns that need to be determined. These four values determine completely the transition zone, $y = p(x)$, $a \leq x \leq X$.

Given X , c_1 , c_2 and R , we can compute $p(x)$ as the Lagrange-Hermite interpolant of the data

$$p^{(j)}(a) = 0, \quad 0 \leq j \leq r, \quad \text{and} \quad p^{(j)}(X) = y^{(j)}(X), \quad 0 \leq j \leq r,$$

where $y(x) = c_2 - \sqrt{R^2 - (x - c_1)^2}$ is the circle. Indeed, this is given in Newton form as

$$p(x) = \sum_{j=0}^{2r+1} p[x_0, \dots, x_j] \prod_{k=0}^{j-1} (x - x_k),$$

with

$$x_0 = x_1 = \dots = x_r = a \quad \text{and} \quad x_{r+1} = \dots = x_{2r+1} = X$$

and, for any values t_1, t_2, \dots, t_m , the divided difference,

$$p[t_1, t_2, \dots, t_m],$$

may be computed from the recurrence

$$p[t_1, \dots, t_m] = \frac{p[t_2, \dots, t_m] - p[t_1, \dots, t_{m-1}]}{t_m - t_1},$$

with

$$p[\underbrace{a, \dots, a}_{\text{multiplicity } j+1}] := 0, \quad 0 \leq j \leq r$$

and

$$p[\underbrace{X, \dots, X}_{\text{multiplicity } j+1}] := \frac{y^{(j)}(X)}{j!}, \quad 0 \leq j \leq r,$$

where again $y(x) = c_2 - \sqrt{R^2 - (x - c_1)^2}$ is the circle.

Note, however, that this defines $p(x)$ as a polynomial of degree $2r + 1$ exceeding our claimed degree $2r - 1$ by 2. Hence, the first two of our equations are that $p(x)$ is actually of degree $2r - 1$, i.e., its two leading coefficients are zero. More specifically, from the Newton form,

$$p[\underbrace{a, a, \dots, a}_{r+1 \text{ copies}}, \underbrace{X, X, \dots, X}_{r+1 \text{ copies}}] = 0 \tag{7}$$

and

$$p[\underbrace{a, a, \dots, a}_{r+1 \text{ copies}}, \underbrace{X, X, \dots, X}_r] = 0. \tag{8}$$

The third equation is that the length of the transition is specified to be L_t , i.e.,

$$\int_a^X \sqrt{1 + (p'(x))^2} dx = L_t. \tag{9}$$

Note that this integral has to be estimated numerically.

Finally, the fourth equation is that the remainder of the circular arc—from $x = X$ to the apex $x = c_1 + R$ —have length L_a . This is easily accomplished. The two endpoints of the circular arc

are $(X, y(X))$ and $(c_1 + R, c_2)$ giving a circular segment of angle θ , say, between the two vectors connecting these points to the centre, i.e., $\langle X - c_1, y(X) - c_2 \rangle$ and $\langle R, 0 \rangle$. Then,

$$\cos(\theta) = \frac{\langle X - c_1, y(X) - c_2 \rangle \cdot \langle R, 0 \rangle}{\| \langle X - c_1, y(X) - c_2 \rangle \|_2 \| \langle R, 0 \rangle \|_2} = \frac{X - c_1}{R}.$$

Hence the fourth equation is

$$R \cos^{-1} \left(\frac{X - c_1}{R} \right) = L_a. \quad (10)$$

Together, equations (7), (8), (9) and (10) form a system of four nonlinear equations in four unknowns, c_1 , c_2 , R and X , determining a C^r transition given by $p(x)$, a polynomial of degree $2r - 1$, satisfying the design parameters.

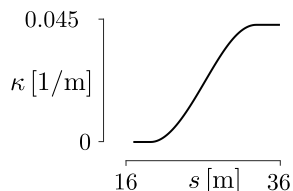


Figure 5: Transition zone track curvature, κ , as a function of distance, s , which — in contrast to Figure 4 — exhibits a smooth (C^1) transition between the zero curvature of the straight and the $1/R$ curvature of the circular arc

For the velodrome under consideration, and a Bloss C^3 transition, with curvature C^1 , we obtain $c_1 = 25.7565$ m, $c_2 = 23.5753$ m, $R = 23.3863$ m and $X = 32.3988$ m, which — as expected — are similar to values obtained in Section 2.1. The corresponding trajectory curvature is shown in Figure 5.

Returning to the quote on page 6, the requirement of differentiability of the trajectory traced by bicycle wheels, which is expressed in spatial coordinates, is a consequence of a dynamic behaviour, which is expressed in temporal coordinates, namely, the requirement of smoothness of the derivative of acceleration, which is commonly referred to as a jolt. In other words, a natural motion of the bicycle-cyclist system, which is laterally unconstrained, ensures that the third temporal derivative of position is smooth; the black line smoothed by this motion.

2.3 Track-inclination angle

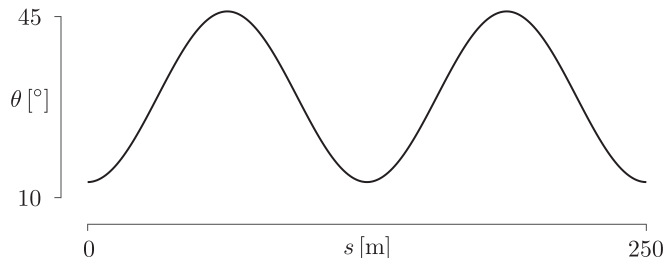


Figure 6: Track inclination, θ , as a function of the black-line distance, s

There are many possibilities to model the track-inclination angle. We choose a trigonometric formula in terms of arclength, which is a good analogy of an actual 250-metre velodrome. The minimum

inclination of 13° corresponds to the midpoint of the straight, and the maximum of 46° to the apex of the circular arc. For a track of length S ,

$$\theta(s) = 29.5 - 16.5 \cos\left(\frac{4\pi}{S}s\right); \quad (11)$$

$s = 0$ refers to the midpoint of the lower straight, in Figure 3, and the track is oriented in the counterclockwise direction. Figure 6 shows this inclination for $S = 250$ m.

It is not uncommon for tracks to be slightly asymmetric with respect to the inclination angle. In such a case, they exhibit a rotational symmetry by π , but not a reflection symmetry about the vertical or horizontal axis. This asymmetry can be modeled by including s_0 in the argument of the cosine in expression (11).

$$\theta(s) = 29.5 - 16.5 \cos\left(\frac{4\pi}{S}(s - s_0)\right); \quad (12)$$

$s_0 \approx 5$ provides a good model for several existing velodromes. Referring to discussions about the London Velodrome of the 2012 Olympics, Solarczyk (2020) writes that

the slope of the track going into and out of the turns is not the same. This is simply because you always cycle the same way around the track, and you go shallower into the turn and steeper out of it.

The last statement is not obvious. For a constant centre-of-mass speed, under rotational equilibrium, the same transition curves along the black line imply the same lean angle.

3 Dissipative forces

A mathematical model to account for the power required to propel a bicycle against dissipative forces is based on

$$P_F = F V, \quad (13)$$

where F stands for the magnitude of forces opposing the motion and V for the centre-of-mass speed. We model the bicycle-cyclist system as undergoing instantaneous circular motion in a horizontal plane, in rotational equilibrium about the instantaneous centre-of-mass velocity, \mathbf{V} .

Even though this model involves several simplifying assumptions, it captures the mechanical behaviour of the system, while allowing us to derive closed-form expressions. Specifically, the assumption of instantaneous circular motion allows us to model motion along a black line of arbitrary geometry in terms of a radius of curvature that varies from point to point. In examining dissipative forces, the assumption that this circular motion occurs in a horizontal plane, although not strictly valid—in particular, since the centre of mass moves along a three-dimensional curve—is an adequate description of a motion whose horizontal displacements have much larger magnitudes than vertical displacements.

Similarly, the assumption of rotational equilibrium about \mathbf{V} is not strictly valid, since—as the cyclist enters and exits a turn—the lean angle increases, reaches a maximum, and decreases. However, this approximation successfully captures the mechanical behaviour of the system, specifically the changing lean of the cyclist, for lap-averaged considerations, discussed in Section 4, below, while again allowing us to derive closed-form expressions.

In view of Figure 7, along the black line, in windless conditions,

$$P_F = \frac{1}{1-\lambda} \left\{ \right. \quad (14a)$$

$$\left(C_{\text{rr}} \underbrace{\overbrace{m g (\sin \theta \tan \vartheta + \cos \theta)}^{F_g}}_N \cos \theta + C_{\text{sr}} \left| \underbrace{\overbrace{\frac{m g \sin(\theta - \vartheta)}{\cos \vartheta}}^{F_g}}_{F_f} \right| \sin \theta \right) v \quad (14b)$$

$$\left. + \frac{1}{2} C_{\text{dA}} \rho V^3 \right\}, \quad (14c)$$

where m is the mass of the cyclist and the bicycle, g is the acceleration due to gravity¹, θ is the track-inclination angle, ϑ is the bicycle-cyclist lean angle, C_{rr} is the rolling-resistance coefficient, C_{sr} is the coefficient of the lateral friction, C_{dA} is the air-resistance coefficient, ρ is the air density and λ is the drivetrain-resistance coefficient. In accordance with the ideal gas law, the air density is

$$\rho = \frac{p M}{R T}, \quad (16)$$

wherein p is the air pressure², M is the molar mass of dry air, R is the gas constant and T is the absolute temperature. We do not include humidity, whose effect on ρ is much smaller than the effect of p , M and T . In expression (14), v is the speed at which the contact point of the rotating wheels moves along the track, which we assume to coincide with the black-line speed. V is the centre-of-mass speed. Since lateral friction is a dissipative force, it does negative work, and the work done against it—as well as the power—are positive. For this reason, in expression (14b), we consider the magnitude, $||$.

Expression (14) gives the instantaneous power required to overcome dissipative forces at a given point along the track, whose design is determined by its radius of curvature, R , and its inclination, θ , which can be viewed as the two independent variables of expression (14) in the sense that if R and θ are constant, so is P_F . R appears in expression (14) implicitly—through expression (25), below—and θ explicitly. Under the assumption of constant V —discussed in Section 5, below—and given the values of m , g and ρ , the two dependent variables are ϑ and v . The four model parameters are λ , C_{rr} , C_{sr} and C_{dA} . Since P_F refers to a given point along the track, to obtain an average of power over an interval, say, a lap, we need to average the values of individual points within a lap.

To formulate summand (14b), we use the relations among the magnitudes of vectors \mathbf{N} , \mathbf{F}_g , \mathbf{F}_{cp} and \mathbf{F}_f , illustrated in Figure 7. In accordance with Newton's second law, for a cyclist to maintain

¹The value of g varies with latitude, ϕ , and altitude, a ,

$$g = g_c (1 + \beta_1 \sin^2 \phi + \beta_2 \sin^2 2\phi) - \left(\frac{2g_0}{r} \right) a, \quad (15)$$

where $g_c = 9.780327 \text{ m/s}^2$, $\beta_1 = 5.30244 \times 10^{-3}$, $\beta_2 = -5.8 \times 10^{-6}$, $g_0 = 9.806257 \text{ m/s}^2$ and $r = 6.371 \times 10^6 \text{ m}$ (e.g., Lowrie, 2007, Sections 2.4.4 and 2.5.4.4). For consistency, to evaluate g in summand (14b), we use expression (15), even though it varies—at the most—by several parts in a thousand, which means that variability of g does not affect the value of P_F in model (14).

²If not measured directly, the air pressure—at altitude a —can be estimated using the isothermal atmosphere assumption with

$$p = p_0 \exp \left(- \frac{g M}{R T} a \right), \quad (17)$$

where p_0 is pressure at sea level (e.g., Bohren and Albrecht, 1998, Chapter 2.2). In general, to evaluate summand (14c), in predicting the value of P_F , we need both expressions (16) and (17). For the accuracy of an *a posteriori* examination, however, only expression (16) could be used, with p obtained by direct measurements.

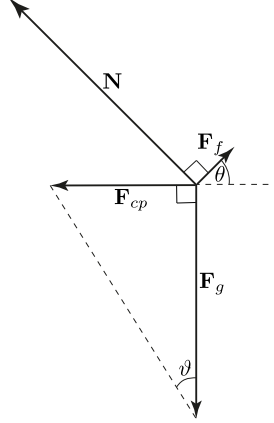


Figure 7: Force diagram: Inertial frame

a horizontal trajectory, the resultant of all vertical forces must be zero,

$$\sum F_y = 0 = N \cos \theta + F_f \sin \theta - F_g. \quad (18)$$

In other words, \mathbf{F}_g must be balanced by the sum of the vertical components of normal force, \mathbf{N} , and the friction force, \mathbf{F}_f , which is parallel to the velodrome surface and perpendicular to the instantaneous velocity. Depending on the centre-of-mass speed and the radius of curvature for the centre-of-mass trajectory, if $\vartheta < \theta$, \mathbf{F}_f points upwards, in Figure 7, which corresponds to its pointing outwards, on the velodrome; if $\vartheta > \theta$, it points downwards and inwards. If $\vartheta = \theta$, $\mathbf{F}_f = \mathbf{0}$. Since we assume no lateral motion, \mathbf{F}_f accounts for the force that prevents it. Heuristically, it can be conceptualized as the force exerted in a lateral deformation of the tires.

For a cyclist to follow the curved bank, the resultant of the horizontal forces,

$$\sum F_x = -N \sin \theta + F_f \cos \theta = -F_{cp}, \quad (19)$$

is the centripetal force, \mathbf{F}_{cp} , whose direction is perpendicular to the direction of motion and points towards the centre of the radius of curvature. According to the rotational equilibrium about the centre of mass,

$$\sum \tau_z = 0 = F_f h \cos(\theta - \vartheta) - N h \sin(\theta - \vartheta), \quad (20)$$

where τ_z is the torque about the axis parallel to the instantaneous velocity, which implies

$$F_f = N \tan(\theta - \vartheta), \quad (21)$$

and h is the centre-of-mass height of the bicycle-cyclist system at $\vartheta = 0$. Substituting expression (21) in expression (18), we obtain

$$N = \frac{m g}{\cos \theta - \tan(\theta - \vartheta) \sin \theta} = m g (\sin \theta \tan \vartheta + \cos \theta). \quad (22)$$

Using this result in expression (21), we obtain

$$F_f = m g (\sin \theta \tan \vartheta + \cos \theta) \tan(\theta - \vartheta) = m g \frac{\sin(\theta - \vartheta)}{\cos \vartheta}. \quad (23)$$

For summand (14c), a formulation of $C_d A \rho V^2 / 2$, therein, is discussed in Appendix A, where we denote it by F_a .

We restrict our study to steady efforts, which—following the initial acceleration—are consistent with a pace of an individual pursuit or the Hour Record. Steadiness of effort is an important consideration in the context of measurements within a fixed-wheel drivetrain, as discussed by Danek et al. (2021, Section 5.2).³ For road-cycling models (e.g., Danek et al., 2021, expression (1))—where curves are neglected and there is no need to distinguish between the wheel speed and the centre-of-mass speed—such a restriction would correspond to setting the acceleration, a , to zero. On a velodrome, this is tantamount to a constant centre-of-mass speed, $dV/dt = 0$.

Let us return to expression (14). Therein, θ is given by expression (11). As shown in Appendix B, the lean angle is

$$\vartheta = \arctan \frac{V^2}{g r_{\text{CoM}}}, \quad (24)$$

where r_{CoM} is the centre-of-mass radius, and—along the curves, at any instant—the centre-of-mass speed is

$$V = v \frac{\overbrace{(R - h \sin \vartheta)}^{r_{\text{CoM}}}}{R} = v \left(1 - \frac{h \sin \vartheta}{R} \right), \quad (25)$$

where R is the radius discussed in Section 2.1 and h is the centre-of-mass height of the bicycle-cyclist system. Along the straights, the black-line speed is equal to the centre-of-mass speed, $v = V$. As expected, $V = v$ if $h = 0$, $\vartheta = 0$ or $R = \infty$. The lean angle, ϑ , is determined by assuming that, at all times, the system is in rotational equilibrium about the line of contact of the tires with the ground; this assumption yields the implicit condition on ϑ , stated in expression (24). Hence, in accordance with expression (25), at any point of the track, V is either equal to or smaller than v .

As illustrated in Figure 7, expressions (24) and (25) assume instantaneous circular motion of the centre of mass to occur in a horizontal plane. Therefore, using these expressions implies neglecting the vertical motion of the centre of mass. Accounting for the vertical motion of the centre of mass would mean allowing for a nonhorizontal centripetal force, and including the work done in raising the centre of mass.

In our model, we also neglect the effect of air resistance of rotating wheels (e.g., Danek et al., 2021, Section 5.5). We consider only the air resistance due to the translational motion of the bicycle-cyclist system. Also, in view of a steady ride and the quantification of average properties per lap, we assume $C_d A$ is constant value, which differs from one cyclist to another but does not vary with speed or track position.

4 Conservative forces

4.1 Mechanical energy

Commonly, in road-cycling models (e.g., Danek et al., 2021, expression (1)), we include $m g \sin \Theta$, where Θ corresponds to a slope; this term represents force due to changes in potential energy associated with hills. This term is not included in expression (14). However—even though we assume the black-line of a velodrome to be horizontal⁴—we wish to account for the power required to increase potential energy to raise the centre of mass upon exiting the curves.

³For a fixed-wheel drivetrain, the momentum of a launched bicycle-cyclist system might result in rotation of pedals whose circumferential speed does not correspond to the amount of force applied by a cyclist at that instant. For variable efforts, this might lead to measurements that do not correspond to the instantaneous power generated by a cyclist. In other words, a measurement—which is the product of applied force and the pedal speed—need not correspond to the power generated at that instant.

⁴In accordance with the UCI regulations (UCI, 2021), the black line is a curve located twenty centimetres from the inside edge of the track in the outward-normal direction. Since this edge is horizontal and the track—in accordance with the UCI regulations—is a ruled surface with varying inclination angle, the black line deviates slightly from a

In Section 3, we assume the cyclist’s centre of mass to travel in a horizontal plane. This is a simplification, since the centre of mass follows a three-dimensional trajectory, lowering while entering a turn and rising while exiting it. We cannot use the foregoing assumption to calculate—from first principles—the change in the cyclist’s potential energy, even though this approach allows us to calculate the power expended against dissipative forces, which is dominated by the power expended against air resistance, which is proportional to the cube of the centre-of-mass speed, V . Along the transition curves, \mathbf{V} has both horizontal and vertical components, and we are effectively neglecting the latter. The justification for doing so—in Section 3—is that the magnitude of the horizontal component, corresponding to the cyclist’s forward motion, is much larger than that of the vertical component, corresponding to the up and down motion of the centre of mass. In Section 4.3, below, we calculate the change in the cyclist’s potential energy instead using the change in the lean angle, whose values are obtained from the assumption of instantaneous rotational equilibrium

Since dissipative forces, discussed in Section 3, are nonconservative, the average power expended against them depends on the details of the path traveled by the cyclist, not just on its endpoints. For this reason, to calculate the average power expended against dissipative forces, we require a detailed model of the cyclist’s path to calculate the instantaneous power. Instantaneous power is averaged to obtain the average power expended against dissipative forces over a lap. This is not the case for calculating the average power needed to increase the cyclist’s mechanical energy. Provided this increase is monotonic, the change in mechanical energy—and therefore the average power—does not depend on the details of the path traveled by the cyclist, but only on its endpoints. In brief, the path dependence of work against dissipative forces requires us to examine instantaneous motion to calculate the associated average power, but the path independence of work to change mechanical energy makes the associated average power independent of such an examination. Thus, as discussed in Appendix C, to allow for comparison of power predictions and measurements, we cannot restrict the power expended to increase mechanical energy to the values along transition curves. Notably, as shown in that appendix, power estimates need to be evaluated for a lap average.

4.2 Kinetic energy

To discuss the effects of mechanical energy, let us consider a bicycle-cyclist system whose centre-of-mass, at a given instant, moves with speed V_1 along the black line whose curvature is R_1 . Neglecting the kinetic energy of the rotating wheels, we consider the kinetic energy of the system due to the translational motion of the centre of mass,

$$K = \frac{1}{2} m V^2 .$$

A bicycle-cyclist system is not purely mechanical; in addition to kinetic and potential energy, the system possesses internal energy in the form of the cyclist’s chemical energy. When the cyclist speeds up, internal energy is converted into kinetic. However, the converse is not true: when the cyclist slows down, kinetic energy is not converted into internal. Thus, to determine the work the cyclist does to change kinetic energy, we should consider only the increases. If the centre-of-mass speed increases monotonically from V_1 to V_2 , the work done is the increase in kinetic energy,

$$\Delta K = \frac{1}{2} m (V_2^2 - V_1^2) . \tag{26}$$

horizontal plane (Stanoev, 2022). Fitton and Symons (2018) include—in their numerical model—the deviation of the black line from a horizontal plane; they do so based on theodolite measurements.

For our model, the minimum track inclination, $\theta_{\min} = 13^\circ$, corresponds to the midpoint of the straight, and the maximum of $\theta_{\max} = 46^\circ$ to the apex of the circular arc. Thus, the change in the black-line height is $0.2(\sin \theta_{\max} - \sin \theta_{\min}) = 0.1 \text{ m}$. Hence, since this change is small in comparison to the length over which it takes place, we assume the black line to be within a horizontal plane.

An analogous deviation of the red line is noticeable with a naked eye, and even more so, of the blue line, which—in a manner similar to the black line—are located at fixed distances from the inside edge.

The stipulation of a monotonic increase is needed due to the nonmechanical nature of the system, with the cyclist doing positive work—with an associated decrease in internal energy—when speeding up, but not doing negative work—with an associated increase in internal energy—when slowing down.

In the case of a constant centre-of-mass speed, $\Delta K = 0$. Otherwise, for instance, in the case of a constant black-line speed (e.g., Bos et al., 2021, Appendix A, Figure A.1), the increase of V occurs twice per lap, upon exiting a curve; hence, the corresponding increase in kinetic energy is $\Delta K = m (V_2^2 - V_1^2)$. The average power, per lap, required for this increase is

$$\bar{P}_K = \frac{1}{1 - \lambda} \frac{\Delta K}{t_\odot}, \quad (27)$$

where t_\odot stands for the laptime. Since, for a constant centre-of-mass speed, $\Delta K = 0$, no power is expended to increase kinetic energy, $P_K = 0$.

4.3 Potential energy

Let us determine the work—and, hence, average power, per lap—performed by a cyclist to change the potential energy,

$$U = m g h \cos \vartheta.$$

Since we assume a model in which the cyclist is instantaneously in rotational equilibrium about the black line, only the increase of the centre-of-mass height is relevant for calculating the increase in potential energy, and so for obtaining the average power required for the increase. Since the lean angle, ϑ , depends on the centre-of-mass speed, V , as well as on the radius of curvature, R , of the black line, ϑ —and therefore the height of the centre of mass—changes if either V or R changes. The work done is the increase in potential energy resulting from a monotonic decrease in the lean angle from ϑ_1 to ϑ_2 ,

$$\Delta U = m g h (\cos \vartheta_2 - \cos \vartheta_1).$$

In the case of a constant centre-of-mass speed, as well as of constant black-line speed,

$$\Delta U = 2 m g h (\cos \vartheta_2 - \cos \vartheta_1),$$

since—in either case—the bicycle-cyclist system straightens twice per lap, upon exiting a curve. The average power, per lap, required for this increase of potential energy is

$$\bar{P}_U = \frac{1}{1 - \lambda} \frac{\Delta U}{t_\odot}. \quad (28)$$

The same considerations—due to the nonmechanical nature of the system—apply to the work done to change potential energy as to that done to change kinetic energy. The cyclist does positive work—with an associated decrease in internal energy—when straightening up, but not negative work—with an associated increase in internal energy—when leaning into the turn.

As stated in Section 4.1, while we neglect the vertical motion of the centre of mass to calculate, with reasonable accuracy, the power expended against dissipative forces, this approach cannot capture the changes in the cyclist’s potential energy along the transition curves. Instead, herein, we calculate these changes starting from the assumption of instantaneous rotational equilibrium and the resulting decrease in lean angle while exiting a turn. Viewed from the noninertial reference frame of a cyclist following a curved trajectory, the torque causing the lean angle to decrease and potential energy to increase is the fictitious centrifugal torque. This torque arises from the speed of the cyclist, which is in turn the result of the power expended on pedaling. Therefore it follows that the increase in

potential energy is subject to the same drivetrain losses as the power expended against dissipative forces and to increase kinetic energy; hence, the presence of λ in expression (28).

Returning to the first paragraph of Section 4.1, we conclude that the changes in potential energy discussed herein are different from the changes associated with hills. When climbing a hill, a cyclist does work to increase potential energy. When descending, at least a portion of that energy is converted into kinetic energy of forward motion. This is not the case with the work the cyclist does to straighten up. When the cyclist leans, potential energy is not converted into kinetic energy of forward motion. Likewise, for a cyclist straightening up coming out of a turn, kinetic energy of forward motion is not simply converted into potential energy. For example, in the case of constant black-line speed, as the cyclist straightens, the centre of mass both speeds up and is raised. Therefore both kinetic and potential energies increase, meaning one cannot be converted into the other. Instead, the rider performs work to increase both. Similarly, for a cyclist leaning into a turn at constant black-line speed, both kinetic and potential energies decrease, again meaning one cannot be converted into the other. In general, since the bicycle and cyclist do not form a purely mechanical system, the decrease in mechanical energy cannot be converted into an increase in the cyclist's internal energy.

In the case of constant centre-of-mass speed, which we consider in the remainder of this article, \bar{P}_U is equal to the additional power required to maintain constant V along the transition curve, upon leaving a circular arc. Along the arcs, v is increased, hence $V < v$ —as shown in Figure 8, on page 17—and, thus conceptually, \bar{P}_U corresponds to work done to bring both speeds together by the end of the transition curve, since $V = v$, along the straights. Let us emphasize that—according to our model, wherein we represent a bicycle-cyclist system by its centre of mass and neglect the kinetic energy of spinning wheels—the increase of v is only a consequence of the inward lean and does not entail any increase of kinetic energy, since V remains constant.

Furthermore, as discussed in Appendix C, instantaneous values of P_U do not yield an empirically adequate model. Consequently, in expression (28), we take \bar{P}_U to be the laptime average. We can do so since the work to straighten up—which within our model is confined to the transition curve—is performed against a conservative force and, hence, depends only on the endpoints of the lean—the maximum along the arcs and the minimum along the straights—not on the evolution of its intermediate values.

5 Constant centre-of-mass speed

5.1 Formulation

In accordance with expression (14), let us find the instantaneous values of P , under the assumption of a constant centre-of-mass speed, V . This assumption is consistent with constraining our attention to steady rides and with examining its motion in terms of the centre of mass.

Stating expression (25), as

$$v = V \frac{R}{R - h \sin \vartheta}, \quad (29)$$

we write expression (14) as

$$P_F = \frac{V}{1 - \lambda} \left\{ \frac{1}{2} C_d A \rho V^2 + \left(C_{rr} m g (\sin \theta \tan \vartheta + \cos \theta) \cos \theta + C_{sr} \left| m g \frac{\sin(\theta - \vartheta)}{\cos \vartheta} \right| \sin \theta \right) \frac{R}{R - h \sin \vartheta} \right\}. \quad (30)$$

Equation (24), namely,

$$\vartheta = \arctan \frac{V^2}{g(R - h \sin \vartheta)},$$

can be solved for ϑ —to be used in expression (30)—given V , g , R , h ; along the straights, $R = \infty$ and, hence, $\vartheta = 0$; along the circular arcs, R is constant, and so is ϑ ; along transition curves, the radius of curvature changes monotonically, and so does ϑ . Along these curves, the radii are given by solutions of equations discussed in Section 2.1 or in Section 2.2.

The values of θ are given— at discrete points— from expression (11), namely,

$$\theta(s) = 29.5 - 16.5 \cos\left(\frac{4\pi}{S}s\right).$$

The values of the bicycle-cyclist system, h , m , C_dA , C_{rr} , C_{sr} and λ , are provided, and so are the external conditions, g and ρ .

Under the assumption of a constant centre-of-mass speed, V , there is no power used to increase the kinetic energy, only the power, \overline{P}_U , used to increase the potential energy. The latter is obtained by expression (28), where the pertinent values of ϑ for that expression are taken from model (30).

5.2 Numerical example

5.2.1 Input and output

To examine the model, let us consider the following values: the Hour Record, which at the time of this article is 56 792 m and which— following the initial laptime of 24 s and as discussed in Appendix D— corresponds to subsequent laptimes of 15.8113 s and, hence, to the black-line speed of $v = 15.8115$ m/s, the bicycle-cyclist mass $m = 97$ kg, altitude and latitude of Grenchen, Switzerland, for which, in accordance with expression (15), $g = 9.80625$ m/s², measured air density $\rho = 1.12$ kg/m³, centre-of-mass height $h = 1.1$ m, $C_dA = 0.184$ m², $C_{rr} = 0.0015$, $C_{sr} = 0.002$ and $\lambda = 0.015$.

To model the Tissot velodrome in Grenchen, we use expression (11), where the track inclination varies from 13°, at the midpoint of the straight, to 46° at the apex of the circular arc. Also, as discussed in Section 2.1, the half-length of the straight is 19 m, the transition curve is 13.5 m and the remaining portion of the arc— whose radius is 23.3863 m— is 30 m; these segments constitute a quarter of the 250-metre track. We use the C^3 transition curve, discussed in Section 2.2.

To evaluate the power of the bicycle-cyclist system, we discretize the black line using 501 evenly spaced points. For each point, we compute numerically the values of V and ϑ that satisfy lean-angle expression (24), which we use in expression (29) to obtain v . We use these values, together with track inclination (11), in model (30). Aspects of such computations are detailed in Appendix C.

The average power per lap— excluding the initial lap and assuming a constant centre-of-mass speed, V , afterwards— is $\overline{P}_\cup = 459.7192$ W, which is the sum of $\overline{P}_F = 416.4016$ W and $\overline{P}_U = 43.3177$ W; 90.5774 % of power is used to overcome dissipative forces and, hence, 9.4226 % to increase potential energy. The corresponding centre-of-mass speed is $V = 15.5010$ m/s, thus, following summand (14c), we calculate that 389.6292 W of \overline{P}_F is used to overcome the air resistance; the remainder of \overline{P}_F is used to overcome the other three dissipative forces, expressed in terms of λ , C_{rr} and C_{sr} .

In accordance with expression (29) and as shown in Figure 8, during each lap, the instantaneous black-line speed, v , varies by 3.5830 %, since, along the straights, $\vartheta = 0^\circ$ and, hence, $v = V = 15.5010$ m/s, and, along the curves— where, in accordance with expression (24), $\vartheta = 47.3422^\circ$ — $v = 16.0564$ m/s. Such an increase of the black-line speed along the curves agrees

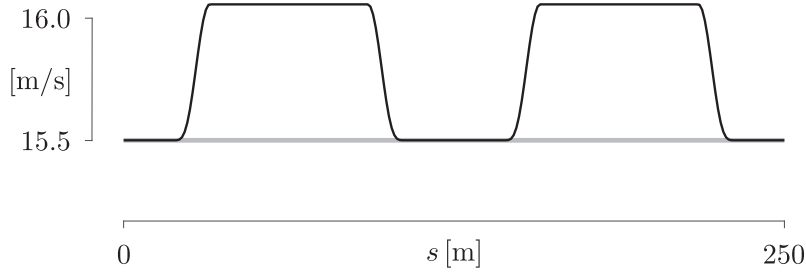


Figure 8: Instantaneous black-line (black) and centre-of-mass (grey) speeds

with empirical results. Within the model, under the assumption of instantaneous rotational equilibrium, the changes of the lean angle, ϑ —and, hence, of the black-line speed, v —are limited to the transition curves.

The instantaneous power, P_F , varies only by 3.0087%, which is consistent with a steady effort. In view of constancy of V , summand (14c), which is the power to overcome air resistance, is constant. Summand (14b), which is the power to overcome rolling resistance and the lateral friction, increases slightly along the curve; this summand is a function of the lean angle, ϑ , the black-line speed, v , and the track-inclination angle, θ .

Since the lean angle varies, $\vartheta \in [0^\circ, 47.3422^\circ]$, for each curve, the centre of mass is raised by $1.1 (\cos(0^\circ) - \cos(47.3422^\circ)) = 0.3546$ m. For this Hour Record, which corresponds to 227 completed laps, the centre of mass is raised by $2(227)(0.3546 \text{ m}) = 160.9973$ m. As discussed in Sections 4.2 and 4.3, there is no conversion of potential energy into kinetic energy upon leaning into the curve. Since we model the motion by focusing on the centre of mass, whose speed is constant, the lean—with the corresponding increase of the black-line speed—does not entail an increase of kinetic energy, which remains constant along the entire lap.

5.2.2 Sensitivity

To gain insight into the sensitivity of the model to errors in input parameters, let us consider $m = 97 \pm 1$ kg, $\rho = 1.12 \pm 0.01$ kg/m³, $h = 1.1 \pm 0.05$ m, $C_d A = 0.184 \pm 0.01$ m², $C_{rr} = 0.0015 \pm 0.0005$, $C_{sr} = 0.002 \pm 0.0005$ and $\lambda = 0.015 \pm 0.005$. For the lower limits, we obtain $\bar{P}_\odot = 422.8547$ W, and for the upper limits, $\bar{P}_\odot = 497.4264$ W. The greatest effect is due to $C_d A$, which is consistent with a dominant contribution of summand (14c) to the value of P_F ; if we consider only $C_d A = 0.184 \pm 0.01$ m², we obtain $438.5437 \text{ W} \leq \bar{P}_\odot \leq 480.8947 \text{ W}$.

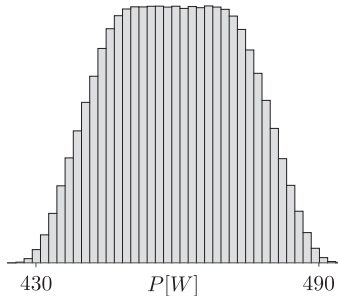


Figure 9: Range of required power obtained by one million Monte-Carlo simulations from uniform distributions of m , ρ , h , $C_d A$, C_{rr} , C_{sr} and λ

To gain insight into the distribution of the output, let us consider a Monte-Carlo simulation by sampling one million values from continuous uniform distributions of m , ρ , h , C_{dA} , C_{rr} , C_{sr} and λ , with the same error ranges as above, to obtain the histogram in Figure 9. The flat top of the histogram is due to the dominant effect of C_{dA} . The sample mean is $\mu = 459.7177$ W and the maximum percentage error is 8.2364%. Since μ is within 0.0003% of the errorless prediction and the histogram is symmetric about the mean, the model is unbiased. Also, the model is stable: small variations in input result in small variations in output. However — in view of possible input errors — the absolute error in power estimates can be substantial.

5.2.3 Different inputs

To gain insight into the effect of significantly different inputs on the required power, let us consider several modifications.

Hour Record: Let the only modification be the reduction of Hour Record to 45 000 m. The required average power reduces to $\bar{P}_{\odot} = 233.1503$ W. Thus, reducing the Hour Record by 21% reduces the required power by about 49%. Let the only modification be the increase of Hour Record to 60 000 m. The required average power increases to $\bar{P}_{\odot} = 540.2455$ W. Thus, increasing the Hour Record by 6% increases the required power by 18%. These results are expected in view of a nonlinear relation between power and speed (e.g., Danek et al., 2021, Section 4, Figure 11).

Altitude: Let the only modification be the increase of altitude to 2600 m, which corresponds to Cochabamba, Bolivia. Following expressions (15) and (16), the corresponding adjustments are $g = 9.7769$ m/s² and $\rho = 0.8754$ kg/m³; hence, the required average power reduces to $\bar{P}_{\odot} = 374.6360$ W.

Temperature: Let the only modification be the reduction of temperature from $T = 27^{\circ}\text{C}$ to $T = 20^{\circ}\text{C}$. Following expression (16), the corresponding adjustment is $\rho = 1.1423$ kg/m³; hence, the required average power increases to $\bar{P}_{\odot} = 467.4985$ W.

Mass: Let the only modification be the reduction of mass to $m = 90$ kg. The required average power reduces to $\bar{P}_{\odot} = 454.6612$ W. In accordance with the formulation in Section 4.3, the proportional reductions of m and \bar{P}_U are equal to one another.

Centre-of-mass height: Let the only modification be the reduction of the centre-of-mass height to $h = 1$ m. The corresponding adjustments are $\bar{P}_F = 418.5302$ W, $\bar{P}_U = 39.3968$ W and $V = 15.5292$ m/s; the required average power decreases to $\bar{P}_{\odot} = 457.9300$ W, which is a consequence of relations among P_F , \bar{P}_U , V and ϑ .

C_{dA} : Let the only modification be the reduction of the air-resistance coefficient to $C_{dA} = 0.175$ m². The required average power reduces to $\bar{P}_{\odot} = 440.6613$ W, which is a consequence of reduction of P_F alone.

Track inclination: Let the only modification be $s_0 = 5$, in expression (12). The required average power is $\bar{P}_{\odot} = 459.7591$ W, which is an increase of less than 0.1%.

Transition curve: Let the only modification be the C^2 , as opposed to C^3 , transition curve. The required average power is $\bar{P}_{\odot} = 459.7886$ W, which is an increase of less than 0.1%.

Segment lengths: Let the only modification be the segment lengths such that the transition curve doubles in length. To maintain $R = 23.3863$ m, we require $L_s = 10.3858$ m, $L_t = 27.0000$ m, $L_a = 25.1142$ m. The required average power is $\bar{P}_\zeta = 460.0787$ W, which is an increase of less than 0.1%.

5.3 Comparison with Fitzgerald et al. (2021)

Let us compare model (14) to Fitzgerald et al. (2021, expression (24)),⁵ which—expressed in our notation—is

$$P'_F = \frac{1}{1-\lambda} \left\{ \frac{1}{2} C_d A \rho V^3 + \left(C_{rr} m g \frac{\cos(\vartheta - \theta)}{\cos \vartheta} + C_{rr} \mu_s m g \frac{\cos(\vartheta - \theta)}{\cos \vartheta} |\vartheta - \theta| \right) v \right\}; \quad (31)$$

it omits changes in potential and kinetic energy, but encompasses the dominant resistive forces for steady riding. Model (31) differs from model (14) by using μ_s , which is a scrubbing resistance (e.g., Lukes et al. (2012)) associated with the assumption of a slight shifting of the handlebars to avoid lateral slipping down the banked track, as opposed to C_{sr} , the coefficient of lateral friction. Both models assume that the bicycle-cyclist system follows the black line. Notably, the same restriction is imposed by Fitton and Symons (2018) to validate their model, even though, in general, they permit the black-line altitude to vary.

For the comparison, we use input parameters specified by Fitzgerald et al. (2021, Section 3). For the cyclist, $h = 1$ m, $m = 75$ kg, $C_d A = 0.2$ m², $C_{rr} = 0.002$, $\mu_s = 0.4125$ /rad, $\lambda = 0.02$. For the environmental conditions, $g = 9.81$ m/s², $\rho = 1.2$ kg/m³. For the velodrome, the length of the track is $S = 250$ m, the turn radius is $R = 23.1950$ m, the length of the transition is $b = 24.9$ m, and the bank angle (Fitzgerald et al. (2021, eq. (19))) is

$$\theta(s) = \left(\frac{\theta_{\max} - \theta_{\min}}{2} \right) \sin \left(\frac{4\pi}{S} s - \frac{\pi}{2} \right) + \frac{\theta_{\max} + \theta_{\min}}{2},$$

where $\theta_{\min} = 13^\circ$ and $\theta_{\max} = 43^\circ$. Using the expressions in Section 2.1, the respective values of the remainder of the quarter circular arc, the half-length of the straight, and the Euler spiral coefficient are

$$c = \frac{\pi R - b}{2} = 23.9846 \text{ m}, \quad a = \frac{S}{4} - b - c = 13.6154 \text{ m}, \quad A = \frac{1}{Rb} = 0.001731 \text{ m}^{-2}.$$

In a manner consistent with our approach, Fitzgerald et al. (2021) specify the instantaneous lean angle and centre-of-mass speed agreeing with expressions (24) and (25)—the numerical experiments assume a steady ride with $V = 16$ m/s, which corresponds to $\bar{v}_\zeta = 16.2890$ m/s and, hence, $t_\zeta = 15.3511$ s. Using these values, together with $C_{sr} = 0.0025$, we compare the models to obtain the lap averages of

$$\bar{P}_F = 531.2604 \text{ W} \quad \text{and} \quad \bar{P}'_F = 534.7769 \text{ W}.$$

Hence, our power to overcome dissipative forces is consistent with Fitzgerald et al. (2021) to within one percent: $100(|\bar{P}_F - \bar{P}'_F|/\bar{P}'_F) = 0.6576\%$, in spite of a different formulation of lateral forces. Also, for either model, during a lap, the power varies by 2.56% and 2.85%, respectively, which agrees with the assumption of a steady ride.

⁵Model (14) appeared in Bos et al. (2020) prior to Fitzgerald et al. (2021).

However, as discussed in Section 4, a velodrome model requires considerations of not only dissipative but also conservative forces. Herein, for either model, $\bar{P}_U = 34.0442 \text{ W}$, which Fitzgerald et al. (2021) do not include; hence, we claim that—for our and the Fitzgerald et al. (2021) model—the required average power per lap is 565.3046 W and 568.8212 W , respectively.

6 Gradual speed increase

Under certain conditions, our model—wherein we assume a constant centre-of-mass speed—can be used to estimate the power required for events of multiple laps, such as individual pursuit and Hour Record, with changing speed. In this section, we show that—even though such an estimate violates the assumption used in Section 5.1—the resulting errors are negligible for pertinent scenarios. To do so, we write expression (27) as

$$(\Delta \bar{P}_K)_i = \frac{1}{1 - \lambda} \frac{(\Delta K)_i}{t_{\odot i}},$$

where

$$(\Delta K)_i = \frac{1}{2} m \left(V_{\odot i+1}^2 - V_{\odot i}^2 \right),$$

which is expression (26) and i is the lap number.

Let us set the time of the first lap to 24 s . The power required for the initial acceleration is not included in our study, which is limited to a steady, or nearly steady, ride of a cyclist who maintains an aerodynamic position. Hence, model results in Table 1 begin with the second lap.

Following the initial lap, to reach $56\,792 \text{ m}$ at the end of the hour—with a constant laptime for all subsequent laps—we require $\bar{v}_{\odot} = 56.9215 \text{ km/h}$, which corresponds to $\bar{P}_{\odot} = 459.7192 \text{ W}$, for each lap.

To reach the same distance—with a linear decrease of laptime,⁶ which is a measurable quantity readily available to a coach during an attempt, shown herein in the third column of Table 1—let us set the average speed at the last lap to $\bar{v}_{\odot n} = 59.0000 \text{ km/h}$. As shown in Appendix D, the average second-lap speed needs to be $\bar{v}_{\odot 2} = 54.9816 \text{ km/h}$.

The average power over all completed laps—excluding the first one—is $\bar{P} = 460.7787 \text{ W}$ and the maximum lap average, which corresponds to the last completed lap is $\bar{P}_{\odot} = 510.5940 \text{ W}$.

Such negative splits are considered desirable to delay the increase of internal body temperature, and were used by Daniel Bigham in his successful attempt in Summer 2022. The average power for negative splits is almost the same as the average lap power of a constant pace. However, the former requires a significantly higher maximum power.

Comparing the values of the last column of Table 1 to the values of the sixth and seventh columns, we see that the amount of power required to accelerate is negligible. Hence, the errors due to violating the assumption of a constant centre-of-mass speed are negligible.

A more direct, albeit less detailed, way to estimate the power required to increase from $\bar{v}_{\odot 2} = 54.9816 \text{ km/h}$, per lap, to $\bar{v}_{\odot n} = 59.0000 \text{ km/h}$, per lap, which correspond to $V = 14.9828 \text{ m/s}$ and $V = 16.0563 \text{ m/s}$, respectively, is to consider the change in kinetic energy, $\Delta K = 1616.0234 \text{ J}$, over time, $(3600 - 24) \text{ s}$, to get $\Delta \bar{P}_K = 0.4588 \text{ W}$, which is consistent with the values of the last column of Table 1. For either estimate, the speed increase requires about 0.1% of the power needed to maintain a constant centre-of-mass speed per lap or of its average over all—but the first—laps.

⁶As illustrated in Figure 10, for small and linear decrease of laptime, the corresponding increase of power is almost linear, even though it is a concave-up curve.

lap [i]	d [m]	t_{\odot} [s]	t [s]	\bar{v} [km/h]	\bar{P}_{\odot} [W]	\bar{P} [W]	V_{\odot} [m/s]	$\Delta\bar{P}_K$ [W]
1	250	24.0000	24.0000	37.5000	—	—	—	—
2	500	16.3691	40.3691	44.5886	415.3158	415.3158	14.9828	0.4009
\vdots	\vdots	\vdots	\vdots	\vdots	\vdots	\vdots	\vdots	\vdots
111	27 750	15.8290	1794.8962	55.6578	458.2101	436.2875	15.4840	0.4582
112	28 000	15.8241	1810.7203	55.6685	458.6306	436.4888	15.4887	0.4588
113	28 250	15.8191	1826.5394	55.6791	459.0515	436.6902	15.4935	0.4594
114	28 500	15.8141	1842.3535	55.6896	459.4730	436.8918	15.4983	0.4599
115	28 750	15.8092	1858.1627	55.7002	459.8950	437.0936	15.5030	0.4605
116	29 000	15.8042	1873.9670	55.7107	460.3175	437.2956	15.5078	0.4611
117	29 250	15.7993	1889.7662	55.7212	460.7405	437.4977	15.5126	0.4617
\vdots	\vdots	\vdots	\vdots	\vdots	\vdots	\vdots	\vdots	\vdots
227	56 750	15.2542	3597.4373	56.7904	510.5940	460.7787	16.0563	—
228	56 792	2.5627	3600.0000	56.7920	—	—	—	—

Table 1: Information corresponding to a constant laptime decrease

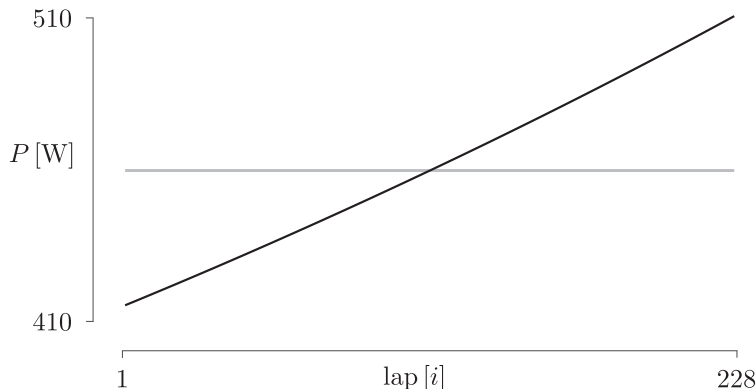


Figure 10: Power required for constant and negative splits

Using the approach described in this section, we generated scenarios for considerations prior to two successful Hour Records in 2022: Daniel Bigham and Filippo Ganna. To do so, we considered several different record predictions and used various speed increases, including cases where the speed for the second half of the hour remained constant, which was the preferred strategy of Daniel Bigham, who has optimized his performance with great attention to details. The speed increase of 4 km/h, illustrated herein, is the highest considered. Hence, for other cases, the errors of estimated power—resulting from violating the assumption of constant V —are even smaller.

7 Conclusions

The mathematical model presented in this article offers the basis for a quantitative study of individual time trials on a velodrome. For a given power, the model can be used to predict laptimes; also, it can be used to estimate the expended power from the recorded times. In the latter case, which is an inverse problem, the model can be used to infer values of parameters, in particular, C_dA , C_{rr} , C_{sr} and λ . For inverse problems, the key measurable quantities are v and P .⁷ V is not a directly

⁷For a fixed-wheel drivetrain, wheel speed can be obtained from cadence, which is a reliable measurement.

measurable quantity; however, in accordance with expression (25), its value is smaller and varies less than v , which further supports the assumption of its being constant, upon which we base the formulation in Section 5.

Let us emphasize that our model is phenomenological. It is consistent with—but not derived from—fundamental concepts. Its purpose is to provide quantitative relations between the model parameters and observables. Its key justification is the agreement between measurements and predictions on which we comment in Appendix E. The relative simplicity of our model—as well as the model by Fitzgerald et al. (2021) and in contrast to Fitton and Symons (2018)—facilitates an empirical examination of specific assumptions. While the accuracy of measurements is insufficient to distinguish between predictions of $\bar{P}_F = 531.2604 \text{ W}$ versus $\bar{P}'_F = 534.7769 \text{ W}$, discussed in Section 5.3, it is possible to obtain empirical evidence for an increase of $\bar{P}_U = 34.0442 \text{ W}$, predicted by our model.

Acknowledgements

We wish to acknowledge Mehdi Kordi, for information on the track geometry and for measurements, used in Section 2 and Appendix E; Daniel Bigham, for fruitful discussions; Elena Patarini, for her graphic support; David Dalton, for his editorial work; Roberto Lauciello, for his artistic contribution; Favero Electronics, for inspiring this study by their technological advances of power meters, notably, IAV (Instantaneous Angular Velocity) Power, discussed by Danek et al. (2021, Appendix A). Following power-meter information from the latest—at the time of this article—successful Hour Record, we pursue the collaboration with Andrea Olivotto of Favero Electronics to enhance the agreement between the model and measurements since, inevitably, both are subject to inaccuracies and errors.

References

- Benham, G. P., Cohen, C., Brunet, E., and Clanet, C. (2020). Brachistochrone on a velodrome. *Proceedings of the Royal Society A*, 476(2238).
- Birkhoff, G. (1950). *Hydrodynamics: A study in logic, fact, and similitude*. Princeton University Press.
- Bohren, C. F. and Albrecht, B. A. (1998). *Atmospheric thermodynamics*. Oxford University Press.
- Bos, L., Slawinski, M. A., Slawinski, R. A., and Stanoev, T. (2020). On modelling bicycle power for velodromes: Part II Formulation for individual pursuits. [arXiv](#), 2009.01162v1 [physics.pop-ph].
- Bos, L., Slawinski, M. A., Slawinski, R. A., and Stanoev, T. (2021). On modelling bicycle power for velodromes: Part II Formulation for individual pursuits. [arXiv](#), 2009.01162 [physics.app-ph].
- Danek, T., Slawinski, M. A., and Stanoev, T. (2021). On modelling bicycle power-meter measurements. [arXiv](#), 2103.09806 [physics.pop-ph].
- Fitton, B. and Symons, D. (2018). A mathematical model for simulating cycling: applied to track cycling. *Sports Engineering*, 21:409–418.
- Fitzgerald, S., Kelso, R., Grimshaw, P., and Warr, A. (2021). Impact of transition design on the accuracy of velodrome models. *Sports Engineering*, 24(23).
- Lowrie, W. (2007). *Fundamentals of Geophysics*. Cambridge University Press, 2nd edition.

- Lukes, R., Hart, J., and Haake, S. (2012). An analytical model for track cycling. Proceedings of the Institution of Mechanical Engineers, Part P: Journal of Sports Engineering and Technology, 226(2):143–151.
- Martin, J. C., Milliken, D. L., Cobb, J. E., McFadden, K. L., and Coggan, A. R. (1998). Validation of a mathematical model for road cycling power. Journal of Applied Biomechanics, 14(3):276–291.
- Solarczyk, M. T. (2020). Geometry of cycling track. Budownictwo i Architektura, 19(2):111–119; doi: 10.35784/bud-arch.1621.
- Stanoev, T. (2022). On technical considerations of UCI-regulated velodrome track design. arXiv, 2207.13556 [physics.pop-ph].
- UCI (2021). Union Cycliste Internationale Regulations. Part III: Track races. Retrieved in 2021 from: <https://www.uci.org/inside-uci/constitutions-regulations/regulations>.
- Underwood, L. and Jermy, M. (2010). Mathematical model of track cycling: the individual pursuit. Procedia Engineering, 2(2):3217–3222.
- Underwood, L. and Jermy, M. (2014). Determining optimal pacing strategy for the track cycling individual pursuit event with a fixed energy mathematical model. Sports Engineering, 17:183–196.

A Air resistance

To formulate summand (14c), we assume that it is proportional to the frontal surface area, A , and to the pressure, p , exerted by air on this area, $F_a \propto pA$, where $p = \rho V^2/2$ has a form of kinetic energy and V is the relative speed of the centre of mass with respect to the air; p is the energy density per unit volume. We can write this proportionality as

$$F_a = \frac{1}{2} C_d A \rho V^2,$$

where C_d is a proportionality constant, which is referred to as the drag coefficient.

A more involved justification for summand (14c) is based on dimensional analysis (e.g., Birkhoff, 1950, Chapter 3). We consider the air-resistance force, which is a dependent variable, as an argument of a function, together with the independent variables, to write

$$f(F_a, V, \rho, A, \nu) = 0;$$

herein, ν is the viscosity coefficient. Since this function is zero in any system of units, it is possible to express it in terms of dimensionless groups, only.

According to the Buckingham theorem (e.g., Birkhoff, 1950, Chapter 3, Section 4)—since there are five variables and three physical dimensions, namely, mass, time and length—we can express the arguments of f in terms of two dimensionless groups. There are many possibilities of such groups, all of which lead to equivalent results. A common choice for the two groups is

$$\frac{F_a}{\frac{1}{2} \rho A V^2},$$

which is referred to as the drag coefficient, and

$$\frac{V \sqrt{A}}{\nu},$$

which is referred to as the Reynolds number. Thus, treating physical dimensions as algebraic objects, we can reduce a function of five variables into a function of two variables,

$$g\left(\frac{F_a}{\frac{1}{2}\rho A V^2}, \frac{V\sqrt{A}}{\nu}\right) = 0,$$

which we write as

$$\frac{F_a}{\frac{1}{2}\rho A V^2} = \varphi\left(\frac{V\sqrt{A}}{\nu}\right),$$

where the only unknown is F_a , and where φ is a function of the Reynolds number. Denoting the right-hand side by C_d , we write

$$F_a = \frac{1}{2}C_d A \rho V^2,$$

as expected. In view of this derivation, C_d is not a constant; it is a function of the Reynolds number. In our study, however — within a limited range of speed — C_d is treated as a constant. Furthermore, since A is difficult to estimate, we include it within this constant, and consider $C_d A$ as a single value, which we denote as $C_d A$.

B Lean angle

In view of Figure 7, the lean angle of a cyclist is

$$\vartheta = \arctan \frac{F_{cp}}{F_g}, \tag{B.1}$$

where the magnitude of the centripetal force is

$$F_{cp} = \frac{m V^2}{r_{\text{CoM}}}, \tag{B.2}$$

and the magnitude of the force of gravity is $F_g = m g$.

To relate F_{cp} and ϑ , we use results (22) and (23) in expression (19), to obtain

$$F_{cp} = N \sin \theta - F_f \cos \theta = m g \tan \vartheta, \tag{B.3}$$

which is tantamount to expression (B.1). Examining expressions (B.2) and (B.3), we see that the lean angle is a function of the centre-of-mass speed and of the radius of curvature for the centre-of-mass trajectory; it is independent of mass or the track inclination.

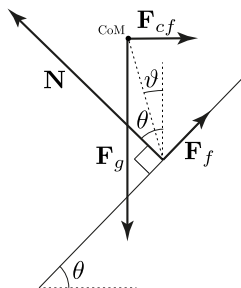


Figure B1: Force diagram: Noninertial frame

Expressions (B.1) and (B.3) imply that the lean angle, ϑ , depends only on the centripetal acceleration of the cyclist's centre of mass and the acceleration of gravity. In other words, the lean angle depends only on the centre-of-mass speed and the radius of curvature of the centre-of-mass trajectory, not on the track inclination, θ , even though both the normal force, stated in expression (22), and the frictional force, in expression (23), do depend on track inclination. However, the θ -dependence cancels out of the centripetal force, stated in expression (B.3), by a seldom used trigonometric identity.

Given the generality of this result, it would be satisfying to obtain it in a manner that explains it in the context of physics. To this end, let us analyze the situation from inside the noninertial frame of the cyclist. Specifically, we consider the frame comoving with the cyclist around a curve, with the cyclist considered as a point mass. We neglect the additional accelerated motion resulting from the rotation of the cyclist about an axis through the centre of mass.

As illustrated in Figure B1 and in contrast to Figure 7, in this noninertial frame, instead of the forces in the horizontal direction summing to the centripetal force, \mathbf{F}_{cp} , the forces in this direction, including the fictitious centrifugal force, $\mathbf{F}_{cf} = -\mathbf{F}_{cp}$, sum to zero. The centrifugal force must be taken to act at the centre of mass, since otherwise the torque about the centre of mass, stated in expression (20), would be affected.

To proceed, we invoke the vector identity,

$$\sum \boldsymbol{\tau} = \mathbf{R}_{\text{CoM}} \times \sum \mathbf{F} + \sum \boldsymbol{\tau}_{\text{CoM}},$$

where $\sum \boldsymbol{\tau}$ is the net torque about an arbitrary point, $\sum \boldsymbol{\tau}_{\text{CoM}}$ is the net torque about the centre of mass, \mathbf{R}_{CoM} is the position vector of the centre of mass, and $\sum \mathbf{F}$ is the net force. From this identity there follows the well-known result that if the net force is zero and the net torque about the centre of mass is zero, the net torque about any other point is also zero. In particular, let us consider the torque about the point of contact of the tires with the surface,

$$\sum \tau_z = h F_g \sin \vartheta - h F_{cf} \sin \left(\frac{\pi}{2} - \vartheta \right) = 0,$$

where h is the centre-of-mass height of the bicycle-cyclist system, from which—considering the magnitudes—it follows that

$$\begin{aligned} \tan \vartheta &= \frac{F_{cf}}{F_g} \\ &= \frac{F_{cp}}{F_g}, \end{aligned} \tag{B.4}$$

where expression (B.4) is equivalent to expressions (B.1) and (B.3). Expression (B.4) manifestly holds whether the curve is banked or unbanked.

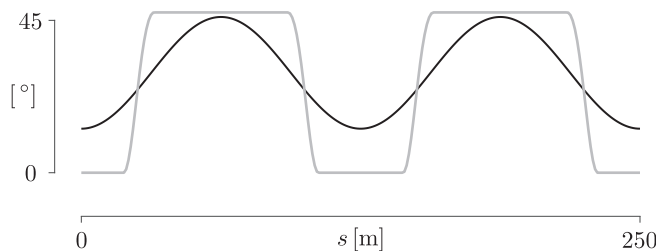


Figure B2: Lean angle, ϑ , (black) and track inclination θ , (grey)

From inside the noninertial frame of the cyclist, the value of the lean angle obtained for specific values of speed and radius is the one that makes the gravitational torque balance the centrifugal torque. In particular, this condition makes no reference to track inclination. As illustrated in Figure B2—in view of instantaneous rotational equilibrium—the lean angle depends on the black-line curvature, shown in Figures 4 and 5, not on track inclination.

C Power for increase of potential energy

In Section 5.2, we consider a bicycle-cyclist system with mass $m = 97$ kg and centre-of-mass height $h = 1.1$ m that completes a lap in $t_{\odot} = 15.8113$ s. Along circular arcs, the cyclist lean angle is $\vartheta = 47.3422^\circ$. Upon leaving a circular arc, the bicycle-cyclist system increases its potential energy along the transition curve, as a result of raising the centre of mass. In accordance with the assumption of instantaneous rotational equilibrium, the change in lean angle is restricted to the transition curve to reach $\vartheta = 0^\circ$, by the beginning of the straight. Thus, along each exiting transition curve, the centre of mass is raised by $\Delta h = h(\cos(0^\circ) - \cos(47.3422^\circ)) = 0.3546$ m. Since it occurs twice per lap, the increase in potential energy per lap is $\Delta U = 2 m g \Delta h = 674.5955$ J. As stated in expression (28), the average power, per lap, required for this increase of potential energy is

$$\bar{P}_U = \frac{1}{1 - \lambda} \frac{\Delta U}{t_{\odot}} = \frac{1}{1 - 0.015} \frac{674.5955 \text{ J}}{15.8113 \text{ s}} = 43.3176 \text{ W}.$$

As shown in Figure C1, if we restrict the increase of potential energy to transition curves, we obtain power values that are inconsistent with empirical evidence; hence, in expression (28) and in Section 5.2, we consider an average per lap.

To obtain values presented in Section 5.2, we use numerical computations along discrete points of the black line. Within each interval along the transition curve, we assume the black-line speed to change linearly,

$$v(s) = v_i + \left(\frac{v_{i+1} - v_i}{s_{i+1} - s_i} \right) (s - s_i).$$

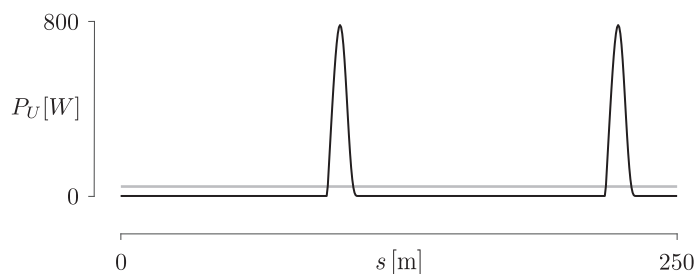


Figure C1: Instantaneous and average power required to raise the centre of mass

Therefore, on the i th interval,

$$v(s) = \frac{ds}{dt}.$$

Separating variables and integrating both sides, we write

$$\int_{t_i}^{t_{i+1}} dt = \int_{s_i}^{s_{i+1}} \frac{ds}{v(s)}.$$

To evaluate the right-hand side, we let

$$u = v(s) \quad \text{and} \quad du = \left(\frac{v_{i+1} - v_i}{s_{i+1} - s_i} \right) ds,$$

which changes the integration limits to v_i and v_{i+1} . Thus, the right-hand side becomes

$$\left(\frac{s_{i+1} - s_i}{v_{i+1} - v_i} \right) \int_{v_i}^{v_{i+1}} \frac{du}{u} = \left(\frac{s_{i+1} - s_i}{v_{i+1} - v_i} \right) \left(\ln(u) \Big|_{v_i}^{v_{i+1}} \right) = \left(\frac{s_{i+1} - s_i}{v_{i+1} - v_i} \right) \ln \left(\frac{v_{i+1}}{v_i} \right).$$

Hence, the time at the end of the i th interval is

$$t_{i+1} = t_i + \left(\frac{s_{i+1} - s_i}{v_{i+1} - v_i} \right) \ln \left(\frac{v_{i+1}}{v_i} \right). \quad (\text{C.1})$$

This expression is valid if $v_{i+1} \neq v_i$; if the black-line speed is constant, $t_{i+1} = t_i + (s_{i+1} - s_i)/v_i$. Using expression (C.1), the power required to increase the potential energy along the i th interval is

$$(P_U)_i = \frac{1}{1 - \lambda} \frac{m g h (\cos \vartheta_{i+1} - \cos \vartheta_i)}{t_{i+1} - t_i}. \quad (\text{C.2})$$

Using input values of Section 5.2, we plot expression (C.2) in Figure C1. $P_U = 0$ everywhere except along the 13.5 m transition curves, where $\cos \vartheta_{i+1} \neq \cos \vartheta_i$; therein, the maximum value of each peak is 783.5231 W.

Thus, we conclude that the assumption of instantaneous rotational equilibrium, which restricts changes of the lean angle to transition curves, does not result in an empirically adequate model for instantaneous values of P_U . Since, in view of conservative forces, P_U depends only on the endpoints of the lean, not on the evolution of its intermediate values, we can consider its average per lap, which is necessary for empirical adequacy of our model.

D Laptimes for gradual speed increase

In Section 6, we examine two pacing strategies for the Hour Record. Following the first lap, one strategy assumes a constant laptime for all subsequent laps whereas the other one assumes a linear decrease of laptime. In this appendix, we derive the expressions used to obtain such laptimes.

During an Hour-Record attempt, a cyclist travels—within one hour, H —a distance, D , on a velodrome, whose length is S . D consists of n laps and r metres of the final incomplete lap. For each complete i th lap, we denote its time by $t_{\odot i}$ and the time along the incomplete lap by t_r ; their sum is one hour,

$$\sum_{i=1}^n t_{\odot i} + t_{\odot r} = H. \quad (\text{D.1})$$

To use this expression, we need to make three assumptions. Since we do not model the initial acceleration—from a standstill to a steady speed—we assign the first laptime. We impose a linear interpolation of laptimes such that

$$t_{\odot i} = t_{\odot 2} + \left(\frac{t_{\odot n} - t_{\odot 2}}{n - 2} \right) (i - 2), \quad \text{for } i \in [2, n]. \quad (\text{D.2})$$

We assume the speed along the incomplete lap to be the speed of the n th lap; hence,

$$t_{\odot r} = \left(\frac{r}{S} \right) t_{\odot n}. \quad (\text{D.3})$$

Using expressions (D.2) and (D.3) in expression (D.1), we write

$$t_{\odot 1} + \sum_{i=2}^n \left(t_{\odot 2} + \left(\frac{t_{\odot n} - t_{\odot 2}}{n-2} \right) (i-2) \right) + \left(\frac{r}{S} \right) t_{\odot n} = H. \quad (\text{D.4})$$

As an aside, let us turn our attention to the summation term. Its lower limit is not equal to one. However, let us invoke a fact that

$$\sum_{i=1}^n c = nc \quad \text{and} \quad \sum_{i=1}^n i = \frac{n(n+1)}{2},$$

where c is a constant value. Then, to evaluate summations with variable lower limits, where $b > a > 1$ and $a, b \in \mathbb{N}$, we write

$$\sum_{i=a}^b c = \left(\sum_{i=1}^b c \right) - \left(\sum_{i=1}^{a-1} c \right) = bc - (a-1)c = (b-a+1)c \quad (\text{D.5})$$

and

$$\sum_{i=a}^b i = \left(\sum_{i=1}^b i \right) - \left(\sum_{i=1}^{a-1} i \right) = \frac{b(b+1)}{2} - \frac{(a-1)(a-1+1)}{2} = \frac{b(b+1) - (a-1)a}{2}. \quad (\text{D.6})$$

Hence, we evaluate the summation in expression (D.4) with the following steps,

$$\begin{aligned} \sum_{i=2}^n \left(t_{\odot 2} + \left(\frac{t_{\odot n} - t_{\odot 2}}{n-2} \right) (i-2) \right) &= \sum_{i=2}^n t_{\odot 2} + \left(\frac{t_{\odot n} - t_{\odot 2}}{n-2} \right) \left(\sum_{i=2}^n i - \sum_{i=2}^n 2 \right) \\ &\quad \text{(distributive property)} \\ &= (n-1)t_{\odot 2} + \left(\frac{t_{\odot n} - t_{\odot 2}}{n-2} \right) \left(\frac{n(n+1) - 2}{2} - (n-1)(2) \right) \\ &\quad \text{(identities (D.5) and (D.6))} \\ &= (n-1)t_{\odot 2} + \left(\frac{t_{\odot n} - t_{\odot 2}}{n-2} \right) \left(\frac{(n-1)(n-2)}{2} \right) \\ &\quad \text{(simplify and factor)} \\ &= (n-1) \left(\frac{t_{\odot 2} + t_{\odot n}}{2} \right). \quad (\text{D.7}) \end{aligned}$$

Returning to equation (D.4) and using result (D.7), we solve for t_2 ,

$$t_{\odot 2} = \frac{2(H - t_1)}{n-1} - \left(1 + \frac{2r}{(n-1)S} \right) t_{\odot n}. \quad (\text{D.8})$$

If $t_{\odot n} = t_{\odot 2}$, which corresponds to a constant-pace strategy, expression (D.8) simplifies to

$$t_{\odot 2} = \frac{S(H - t_1)}{r + (n-1)S}, \quad (\text{D.9})$$

which is the laptime for the second—and all subsequent—laps. In Section 6, $D = 56\,792$ m, $S = 250$ m, $H = 3600$ s and $t_1 = 24$ s. Hence, using modular arithmetic, we calculate

$$r = D \bmod S = 56\,792 \text{ m} \bmod 250 \text{ m} = 42 \text{ m}$$

and

$$n = \frac{D - r}{S} = \frac{56\,792\text{ m} - 42\text{ m}}{250\text{ m}} = 227.$$

Thus, expression (D.9) results in

$$t_{\odot 2} = \frac{(250\text{ m})(3600\text{ s} - 24\text{ s})}{(42\text{ m}) + (227 - 1)(250\text{ m})} = 15.8113\text{ s},$$

which corresponds to $\bar{v}_{\odot 2} = 56.9215\text{ km/h}$ and which remains the same for all subsequent laps.

For an increasing-pace strategy, we need to choose $\bar{v}_{\odot n}$, the average speed on the final lap, to obtain the corresponding laptime, $t_{\odot n} = S/\bar{v}_{\odot n}$. Letting $\bar{v}_{\odot n} = 59.0000\text{ km/h} = 16.3889\text{ m/s}$, we obtain $t_{\odot n} = 15.2542\text{ s}$, which appears in the penultimate row of Table 1, on page 21. Hence, according to expression (D.8),

$$t_{\odot 2} = \frac{2(3600\text{ s} - 24\text{ s})}{227 - 1} - \left(1 + \frac{2(42\text{ m})}{(227 - 1)(250\text{ m})}\right) (15.2542\text{ s}) = 16.3691\text{ s},$$

which appears in the second row of Table 1 and which corresponds to $\bar{v}_{\odot 2} = 54.9816\text{ km/h}$.

E Empirical adequacy

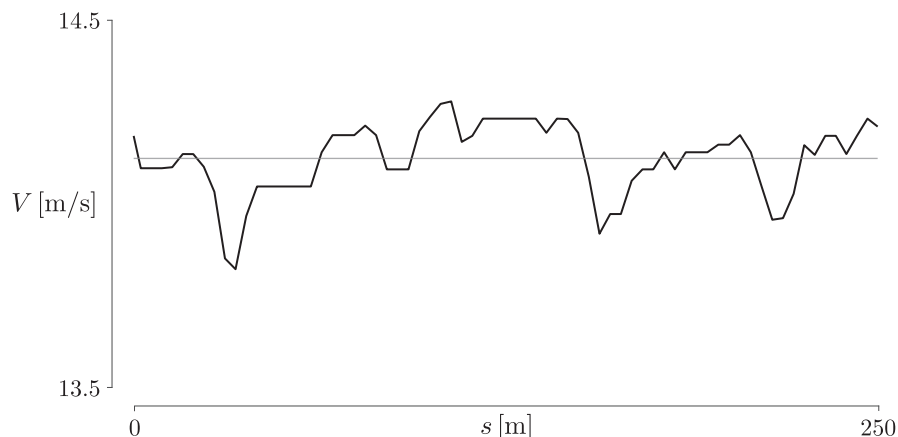


Figure E1: Centre-of-mass speed and its average obtained from measurements

To gain insight into the empirical adequacy of the model, let us compare its predictions with measurements made by Mehdi Kordi (*pers. comm.*, 2022). Therein, we consider a steady lap, whose average power is $\bar{P} = 402.8143\text{ W}$. Other values are $m = 80\text{ kg}$, $h = 1\text{ m}$, $g = 9.8126\text{ m/s}^2$, $\rho = 1.1950\text{ kg/m}^3$. The resistance coefficients are estimated to be $C_d A = 0.20\text{ m}^2$, $C_{rr} = 0.0025$, $C_{sr} = 0.0035$ and $\lambda = 0.020$. Hence, $\bar{P} = \bar{P}_F + \bar{P}_U = 375.3495\text{ W} + 25.7459\text{ W} = 401.0954\text{ W}$, which agrees with the measured power. \bar{P}_F alone would be an underestimate.

Also, measurements allow us to comment on the assumption of a constant centre-of-mass speed, V . Instantaneous V , obtained from measurements, is shown in Figure E1. Its mean is $\bar{V} = 14.1211\text{ m/s}$ and its standard deviation is 0.0964 m/s . Only slight deviations from the mean and lack of a spatial pattern in instantaneous V support the aforementioned assumption. These deviations might be mainly due to measurement errors.